Journal of Engineering Research and Reports

Volume 26, Issue 8, Page 218-235, 2024; Article no.JERR.120556
ISSN: 2582-2926

Study and Optimization of Three-Dimensional Free Bending Forming Law for Metal Hollow Members

Yang Ao [a*]

[a] *School of Mechanical Engineering, North China University of Water, Zhengzhou, China.*

Author's contribution

The sole author designed, analysed, interpreted and prepared the manuscript.

Article Information

DOI: https://doi.org/10.9734/jerr/2024/v26i81240

Open Peer Review History:
This journal follows the Advanced Open Peer Review policy. Identity of the Reviewers, Editor(s) and additional Reviewers, peer review comments, different versions of the manuscript, comments of the editors, etc are available here: https://www.sdiarticle5.com/review-history/120556

Original Research Article

Received: 28/05/2024
Accepted: 30/07/2024
Published: 01/08/2024

ABSTRACT

In order to study the three-dimensional free bending of metal pipe forming law, to improve the three-dimensional free bending process of metal pipe forming quality, φ12mm × 1mm TP2 copper pipe as the object of study, through the related blank and material properties on the pipe bending and forming the influence of the law found that the smaller the pipe bending radius, the more significant the impact of the wall thickness on the bending radius of the pipe, pipe molding quality decreases with the increase in the wall thickness. The pipe bending radius size is determined by the material modulus of elasticity, yield strength, pipe hardening index and strength factor and other parameters together. The maximum ellipticity of the pipe is related to the material strength, and the wall thickness variation of the pipe is affected by the hardening index n. Orthogonal tests are designed and simulated for five groups of process parameters to obtain the optimum value of each group of parameters and the importance of the five groups of parameters on the pipe forming quality. TP2 copper pipe free bending test, the test results and the simulation results of the bending angle and bending radius of the numerical deviation is less than 5%, the maximum wall thickness reduction rate and the maximum elliptic rate of the pipe deviation value is less than 2%, it can be

**Corresponding author: Email: 1728684497@qq.com;*

Cite as: *Ao, Yang. 2024. "Study and Optimization of Three-Dimensional Free Bending Forming Law for Metal Hollow Members". Journal of Engineering Research and Reports 26 (8):218-35. https://doi.org/10.9734/jerr/2024/v26i81240.*

seen that the finite element simulation can provide a reliable basis for the actual forming test, the optimization results of the improvement of the quality of tube molding and the improvement of the molding mechanism of the test equipment is of great importance in guiding significance.

Keywords: Metal pipes; free-bending; molding law; process optimization.

1. INTRODUCTION

With the processing technology of complex structural hollow members becoming more and more perfect, the application fields of metal hollow members are more and more extensive. For example, they are involved in aviation, aerospace, medical, construction, and home decoration [1]. At the same time, various fields put forward higher requirements for the forming technology of hollow pipes. Compared with the traditional bending process, the pipe free bending process can make the metal hollow components to complete the complex three-dimensional continuous curvature forming, and to ensure higher forming quality under the premise of greatly improving the processing efficiency.

Cheng Xuan [2] investigated the effect of different parameters on the forming of rectangular pipes during free bending. It was shown that as the yield strength, thickness, fillet radius, die clearance, coefficient of friction and fillet radius of the guiding mechanism increased, the rate of change of thickness and cross-section deformation decreased, and the bending radius of the pipe increased. The rate of change of pipe thickness decreases with increase in axial feed rate. Cheng Cheng et al. [3] investigated the effect of friction coefficient on the arc radius, wall thickness change and cross-section deformation of bent pipe. The results revealed that with the increase of the friction coefficient, the radius of the arc gradually decreases, the wall thickness increases more obviously, and the cross-section deformation is serious. Wu et al. [4-5] proposed a new integrated control strategy for 3D pipe bending springback. The bending shape was optimized during the forming process using the DA (displacement adjustment) method and B&T (bending and torsion combination) method, and the formed pipe was discretized to obtain the optimized forming parameters. The sensitivity of rebound to process parameters was analyzed by Fang Jun et al. The results showed that the radius of rebound was more sensitive to the process parameters, while the sensitivity of rebound angle to each process parameter was not significant. [6], and the effects of different loading methods on rebound were investigated, and the results showed that a reasonable selection of the loading index K is conducive to improving the prediction accuracy. Li Tao [7] studied the spiral forming process in three-dimensional free bending and found that the ellipticity of the bent section of the pipe is related to the spiral diameter and pitch, and the outward offset of the neutral layer of the pipe in the bending process decreases with the increase of the spiral diameter. Yu Bo et al. [8] investigated that under the same bending die offset (U) condition, the bending radius (R) of the formed pipe decreased with the decrease of friction coefficient, and the thickening of the wall thickness on the inner side of the bending arc section was more and more obvious, while the phenomenon of thinning of the wall thickness on the outer side of the bending arc section was weakened. Cross-sectional distortion rate with the increase of the friction coefficient shows a tendency to increase and then gradually flatten out.

In this paper, based on the three-axis free bending equipment, TP2 copper tube with φ12mm*1mm is the main research object. To study the influence of relevant blank and material properties on pipe bending and forming, The parameters are analyzed by orthogonal tests to optimize the pipe forming quality, and the validity of numerical simulation is verified by free bending tests.

2. THREE-DIMENSIONAL FREE BENDING MOLDING PRINCIPLE AND MECHANICAL ANALYSIS

The key components of the three-axis free bending and forming equipment are mainly composed of spherical bearings, propulsion mechanism, bending die, guide mechanism and other parts, as shown in Fig. 1. The guide mechanism is stationary and the propulsion mechanism moves at a constant speed along the Z-axis, The spherical bearing moves in the XY plane and the bending die moves and rotates in the XY plane. The pipe is bent arbitrarily in the three-dimensional direction under the joint action of the bending die, the propulsion mechanism and the guiding mechanism.

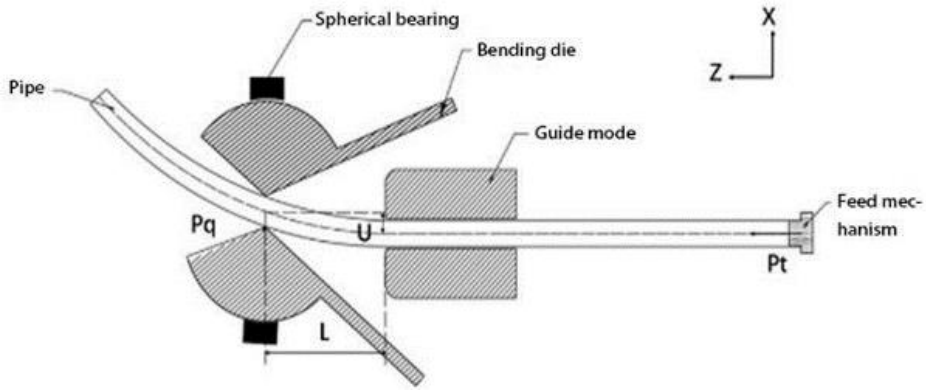

Fig. 1. Structural diagram of triaxial free bending

The larger the bending die eccentricity, the smaller the length of the bending deformation zone, and the smaller the pipe bending limit radius. The bending moment [9] to which the pipe is subjected during bending is:

$$M = P_q L + P_t U \tag{1}$$

where P_q is the thrust of the spherical bearing against the pipe; P_t is the thrust of the propulsion mechanism against the pipe; U is the spherical bearing eccentricity; L is the length of the bending deformation zone.

Three-dimensional free bending mechanical analysis model of pipe based on the principle of metal plastic forming. To simplify the model, the friction between the pipe and the bending die is neglected; the pipe cross-section is always perpendicular to the centerline of the pipe, and the pipe cross-section does not produce distortion when bending; considering that the pipe bends freely under plane strain, circumferential strain $\varepsilon_\varphi = 0$;the bending deformation of the pipe conforms to the volumetric incompressibility condition. In order to avoid the rigor of power function integrals, The pipe material model was modeled using a linear reinforcement model [10], the stress-strain relationships are as follows:

$$\sigma = \sigma_s + D\left(\varepsilon - \varepsilon_S\right) \tag{2}$$

where σ_S is the initial yield strength of pipe; ε_S is the strain corresponding to initial yield strength of pipe; D is the linear hardening factor.

Pipes in the bending deformation process is affected by a combination of factors. The geometric parameters of pipe bending deformation are shown schematically in Fig. 2. In the figure ρ is the radius of curvature at any point of the bend; ψ is the angle between any radius line of the cross-section and the original center layer; R_0 is radius of curvature of the original neutral layer of the bend; R_ξ is radius of curvature of the strain neutral layer of the bend; R_o , R_i is outermost and innermost radii of curvature of the bend; y is the length of the neutral layer spacing between any position of the bend and the bending strain; d_0 , t_0 is original outside diameter and wall thickness of the pipe; d , t is bend the outside diameter and wall thickness of the pipe; σ_θ , ε_θ is pipe tangential stress strain; σ_ρ , ε_ρ is radial stress-strain of the pipe; σ_ψ , ε_ψ is pipe circumferential stress-strain.

Assuming that there is no shear deformation during bending, the stress balance equation can be simplified as:

$$\frac{d\sigma_\rho}{d\rho} + \frac{\sigma_\rho - \sigma_\theta}{\rho} = 0 \tag{3}$$

Based on the assumption of zero strain in the circumferential direction and the incompressible volume condition, the stress in the circumferential direction of the bend cross-section is:

$$\sigma_\psi = \frac{\sigma_\rho + \sigma_\theta}{2} \tag{4}$$

The equivalent force and equivalent strain of the bend are respectively:

$$\bar{\sigma} = \sqrt{\frac{1}{2}\left[\left(\sigma_\rho - \sigma_\theta\right)^2 + \left(\sigma_\theta - \sigma_\psi\right)^2 + \left(\sigma_\psi - \sigma_\rho\right)^2\right]} = \left|\sigma_\theta - \sigma_\rho\right| \tag{5}$$

$$\bar{\varepsilon} = \sqrt{\frac{2}{3}\left(\varepsilon_\rho{}^2 + \varepsilon_\theta{}^2 + \varepsilon_\psi{}^2\right)} = \frac{2}{\sqrt{3}}\left|\varepsilon_\theta\right| \tag{6}$$

Based on a simplified linear reinforced material model, considering tangential compressive stresses due to axial thrust, the equation between the equivalent force and the equivalent strain is:

$$\bar{\sigma} = \frac{\sqrt{3}}{2}\left|\sigma_\psi - \sigma_\rho\right| + \sigma_N \tag{7}$$

Substituting equations (6) and (7) into (4) yields:

$$\frac{\sqrt{3}}{2}\left|\sigma_\psi - \sigma_\rho\right| = \sigma_S - \sigma_N + D\left(\frac{2}{\sqrt{3}}\left|\varepsilon_\theta\right| - \varepsilon_S\right) \tag{8}$$

The transient strain neutral layer of the pipe in the bending process is gradually deflected to the outside under the action of the propulsion force, and the tangential engineering strain of the pipe can be expressed as:

$$\varepsilon_\theta = \frac{\left(R_\xi + y\right)d\theta - R_\xi d\theta}{R_\xi d\theta} = \frac{r\sin\psi - r\sin\beta}{R_0 + r\sin\beta} \tag{9}$$

Joining (4) and (9) gives:

$$\sigma_\theta - \sigma_\rho = \pm\frac{2}{\sqrt{3}}\varepsilon_S\left(1 - \frac{D}{E}\right) - \frac{2}{\sqrt{3}}\sigma_N + \frac{4}{3}D\frac{r\sin\psi - r\sin\beta}{R_0 + r\sin\beta} \tag{10}$$

Substituting equation (10) into equation (3) yields:

$$\begin{aligned} d\sigma_\rho &= \left(\sigma_\theta - \sigma_\rho\right)\frac{d\rho}{\rho} \\ &= \left[\pm\frac{2}{\sqrt{3}}\varepsilon_s\left(1 - \frac{D}{E}\right) - \frac{2}{\sqrt{3}}\sigma_N + \frac{4}{3}D\frac{r\sin\psi - r\sin\beta}{R_0 + r\sin\beta}\right]\frac{d\rho}{\rho} \end{aligned} \tag{11}$$

According to the calculated integration constants, the radial stresses on the inner arc side and outer arc side of the bend are:

$$\begin{aligned} \sigma_{\rho i} &= \frac{2}{\sqrt{3}}\ln\frac{R_i}{\rho}\left[\sigma_S\left(1 - \frac{D}{E}\right) + \frac{2}{\sqrt{3}}\sigma_N\right] \\ &+ \frac{4}{3}D\left(\frac{r\sin\psi - r\sin\beta}{R_0 + r\sin\beta}\ln\rho - \frac{r - r\sin\beta}{R_0 + r\sin\beta}\ln R_i\right) \end{aligned} \tag{12}$$

$$\begin{aligned} \sigma_{\rho 0} &= \frac{2}{\sqrt{3}}\sigma_S\left(1 - \frac{D}{E}\right)\ln\frac{\rho}{R_0} + \frac{2}{\sqrt{3}}\sigma_N\ln\frac{R_0}{\rho} \\ &+ \frac{4}{3}D\left(\frac{r\sin\psi - r\sin\beta}{R_0 + r\sin\beta}\ln\rho - \frac{r + r\sin\beta}{R_0 + r\sin\beta}\ln R_0\right) \end{aligned} \tag{13}$$

The tangential stress at any radius of curvature ρ can be found by substituting equations (12) and (13) into (10):

$$\begin{aligned} \sigma_{\sigma i} &= \left[\frac{2}{\sqrt{3}}\sigma_S\left(1 - \frac{D}{E}\right) + \frac{2}{\sqrt{3}}\sigma_N\right]\left(\ln\frac{R_i}{\rho} - 1\right) \\ &+ \frac{4}{3}D\frac{r\sin\psi - r\sin\beta}{R_0 + r\sin\beta}\left(\ln\rho + 1\right) \\ &- \frac{4}{3}D\frac{r - r\sin\beta}{R_0 + r\sin\beta}\ln R_i \end{aligned} \tag{14}$$

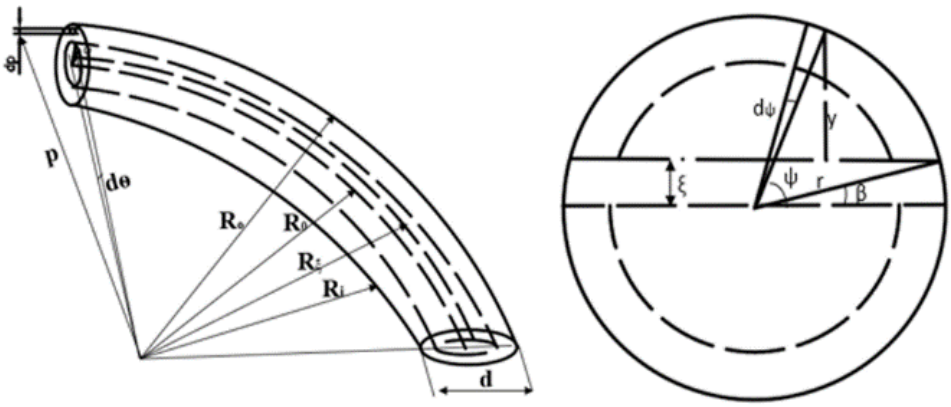

Fig. 2. Mechanical model diagram of elbow

$$\sigma_{\sigma 0} = \frac{2}{\sqrt{3}}\sigma_S\left(1-\frac{D}{E}\right)\left(\ln\frac{\rho}{R_0}+1\right)+\frac{2}{\sqrt{3}}\sigma_N\left(\ln\frac{\rho}{R_0}-1\right) + \frac{4}{3}D\frac{r\sin\psi - r\sin\beta}{R_0 + r\sin\beta}\left(\ln\rho - 1\right) + \frac{4}{3}D\frac{r + r\sin\beta}{R_0 + r\sin\beta}\ln R_0 \quad (15)$$

The radial stress on the inner and outer surfaces of the bend is 0. The equivalent stress on the inner and outer surfaces of the bend is:

$$\overline{\sigma_l} = \left|\frac{2}{\sqrt{3}}\sigma_S\left(1-\frac{D}{E}\right)+\frac{8FL}{\sqrt{3}\pi d_0^{\,2}}+\frac{4}{3}D\frac{r - r\sin\beta}{R_0 + r\sin\beta}\right| \quad (16)$$

$$\overline{\sigma_o} = \left|\frac{4}{\sqrt{3}}\sigma_S\left(1-\frac{D}{E}\right)-\frac{8FL}{\sqrt{3}\pi d_0^{\,2}}+\frac{4}{3}D\frac{r + r\sin\beta}{R_0 + r\sin\beta}\right| \quad (17)$$

Assuming that the axial thrust acts uniformly in the tangential direction of the bend, the tangential stress caused by the axial thrust and bending moment must satisfy the static equilibrium relationship on the bending line, as shown in the following equation:

$$\int_{\pi+\beta}^{2\pi-\beta}\left[\sigma_S\left(1-\frac{D}{E}\right)-\sigma_N+D\frac{r\sin\psi - r\sin\beta}{R_0 + r\sin\beta}\right]r_m t_o d\psi + \int_{-\beta}^{\pi+\beta}\left[-\sigma_S\left(1-\frac{D}{E}\right)-\sigma_N+D\frac{r\sin\psi - r\sin\beta}{R_0 + r\sin\beta}\right]=0 \quad (18)$$

The relationship between the outer wall thickness t_o and inner wall thickness t_i of the pipe and the original wall thickness t_0 is given by:

$$t_o = t_0 - \frac{\Delta t}{2} \quad (19)$$

$$t_i = t_0 + \frac{\sqrt{3}\Delta t}{2} \quad (20)$$

$$\frac{\Delta t}{t_o} = \frac{1+\sin\beta}{\frac{2R_o}{d_o}+\frac{2t_o}{d_o}-\sin\beta} \quad (21)$$

Substituting the above equations into (18) yields the following equation for the strain neutral layer displacement angle and lateral displacement relationship:

$$|\beta| = \frac{\frac{\pi}{2}\left[\frac{\sigma_N}{D}-\frac{\sigma_s}{D}\left(1-\frac{D}{E}\right)\frac{\Delta t}{t_o}\right]\left(\frac{R}{r}-\sin\alpha\right)-\frac{\pi}{2}\sin\beta+\frac{\Delta t}{t_o}\cos\beta}{\frac{\sigma_s}{D}\left[\left(1-\frac{D}{E}\right)-\frac{\Delta t}{t_o}\right]\left(\frac{R}{r}-\sin\alpha\right)-\frac{\Delta t}{t_o}\sin\beta} \quad (22)$$

$$\xi = r\sin|\beta| \quad (23)$$

3. THREE-DIMENSIONAL FREE BENDING FINITE ELEMENT STUDY

3.1 Forming Quality Evaluation Index and Multi-objective Optimization Method Selection

The evaluation criteria for pipe forming quality are wall thickness reduction and ellipticity, which are calculated by the following formulas [11]:

$$\delta = \frac{t - t_{min}}{t}\times 100\% \quad (24)$$

where δ is the wall thickness reduction rate; t is original wall thickness of pipe (mm); t_{min} is the minimum wall thickness of the pipe (mm). Engineering that the bend wall thickness reduction rate should be no more than 10% is qualified [12].

$$\varepsilon = \frac{D_{max} - D_{min}}{D_{max}}\times 100\% \quad (25)$$

where ε is the ellipticity; D_{max} is the maximum cross-sectional diameter of the pipe; D_{min} is the minimum cross-sectional diameter of the pipe. In industrial piping, copper tubing is required to have an ovalization rate of no more than 8%.

In this paper, the efficacy coefficient method was chosen as the multi-objective optimization method for this study [13].

$$\eta_k = \frac{f_{kmax}(X) - f_k(X^k)}{f_{kmax}(X) - f_{kmin}(X)} \quad (26)$$

where $f_{kmax}(X)$ and $f_{kmin}(X)$ are the extremes of $f_k(X)$ under the constraints, while the goodness of the multi-objective program is judged by the magnitude of the total efficacy coefficient, with the best results when η = 1:

$$\eta = \sqrt[q]{\eta_1 \eta_2 \ldots \eta_q} \rightarrow max \quad (27)$$

3.2 Analysis of the Effect of Different Wall Thicknesses of Pipes on the Molding Pattern

TP2 copper tubes with wall thicknesses of 0.5 mm, 1 mm, and 2 mm were selected for simulation. From Fig. 3, it can be seen that in the 0-1s transition section, with the increase of the bending die eccentricity, the bending pipe from the elastic deformation stage gradually transformed to the plastic deformation stage, the pipe in the Z direction of the thrust gradually increased, in the 1s-4s arc section, the pipe in the process of moving the size of the bending moment is unchanged, the pipe is subjected to the Z thrust is also gradually in a stable state. With the increase of wall thickness, the Z-axis thrust force on the pipe also increases gradually.

Different wall thickness of the pipe in the X-axis direction of the thrust shown in Fig. 4, the wall thickness increases so that the pipe in the bending process of the X-axis thrust also gradually increased, wall thickness of 1mm and wall thickness of 2mm pipe between the thrust changes in the range of small, when the wall thickness of 2mm, the maximum X-axis thrust of more than 10,000N at 1s.

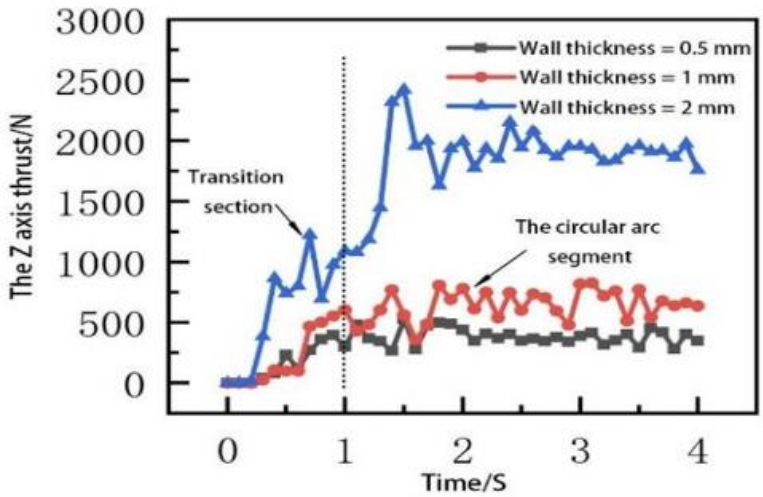

Fig. 3. Variation of z-axis thrust of tube under different wall thickness

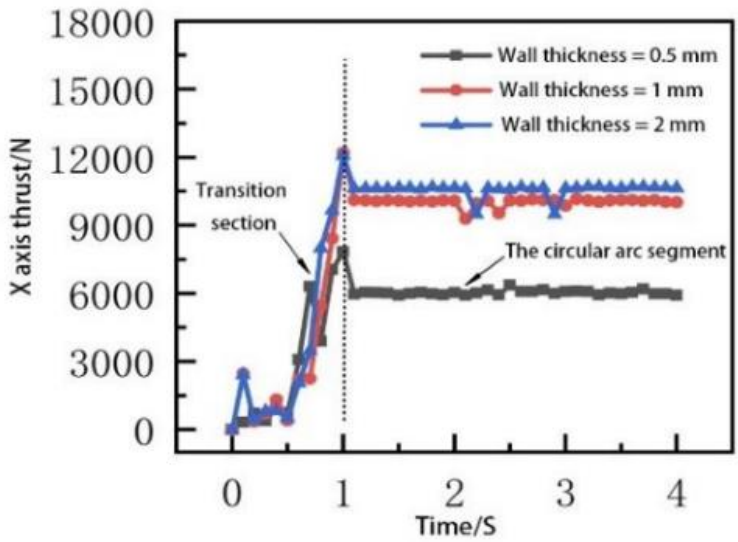

Fig. 4. Variation of x-axis thrust of tube under different wall thickness

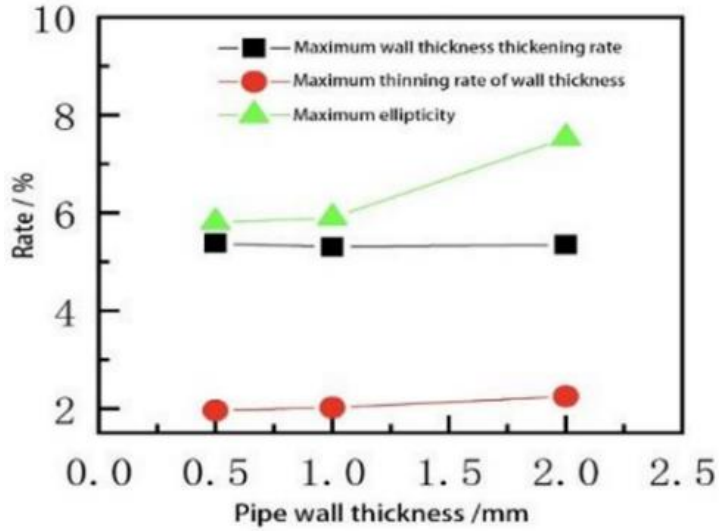

Fig. 5. Relationship between tube change rate and wall thickness

The rate of change of pipe under different wall thicknesses is shown in Fig. 5, the rate of change of wall thickness on the inner and outer sides of the pipe increases with the increase in wall thickness of the pipe, but the magnitude of the change is small, and the ellipticity of the pipe increases with the increase in the thickness of the pipe wall, and a comparison of the 2mm wall thickness pipe and the 0.5mm wall thickness pipe shows that the ellipticity of the 2mm wall thickness pipe increases significantly, more than 7%.

The bending deformation of the pipe at different wall thicknesses is shown in Fig. 6. From the figure, it can be seen that different pipe wall thicknesses also have an effect on the bending radius of the pipe, in which the 2mm wall thickness bending radius is the largest, and the 1mm wall thickness bending radius is the smallest. However, the thicker wall thickness of the pipe in the bending transition section of the ellipticity is relatively large, with the increase of the bending radius, the maximum stress of the pipe is gradually reduced. In order to further investigate the forming law of pipes with different wall thicknesses under different bending radii and bending angles, the bending die eccentricity U=4mm, 6mm, 8mm, 10mm were selected for further study, and the bending radius of the pipe, the maximum wall thickness reduction rate, and the maximum ellipticity under this parameter were analyzed, as shown in Table 1.

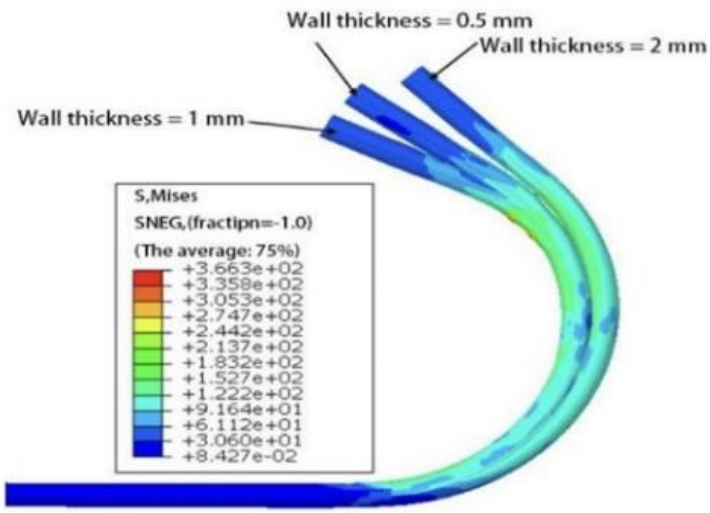

Fig. 6. Bending deformation of tube under different wall thickness

Table 1. Tube forming parameters under different wall thickness and different eccentricity of bending die

Wall thickness h（mm）	Bending die eccentricity U（mm）	Bending radius R（mm）	Maximum wall thickness reduction（%）	Maximum ellipticity（%）
0.5	4	162.42	1.74	3.32
	6	130.88	1.96	5.77
	8	98.48	2.72	6.58
	10	67.79	3.88	7.89
1	4	160.81	1.77	4.46
	6	136.46	2.02	5.16
	8	106.60	2.91	7.72
	10	76.65	4.42	8.69
2	4	164.32	1.79	5.21
	6	143.82	2.13	7.68
	8	114.91	2.96	10.42
	10	85.16	4.68	12.03

When the bending die eccentricity is small, the difference between the bending radius of different wall thicknesses of the pipe is small and shows no regular change, when the eccentricity is larger, the bending radius of the three wall thicknesses of copper pipe bending radius difference is more obvious. The larger the pipe wall thickness, the larger the bending moment required under the same radius, the pipe bending moment required by the bending mold eccentricity U and pipe bending deformation zone length L together, the equipment in the work of the U and L value is unchanged, different wall thickness of pipe bending bending process by the bending moment size is equal, so the larger the wall thickness, the larger the bending radius of the pipe. In the small eccentricity pipe wall thickness and bending radius without significant regular changes may be due to the pipe bending angle is small, bending rebound, friction changes and other factors on the pipe bending radius of the accuracy of a greater impact. Under the same eccentricity, the pipe wall thickness thinning rate is positively correlated with the wall thickness, and under the large eccentricity, the maximum wall thickness thinning rate of thick-walled pipes increases more significantly. In addition, the maximum wall thickness reduction rate of thick-walled pipes is higher than that of thin-walled pipes under large eccentricity, but the maximum wall thickness reduction rate is still within the qualified range, so it can be seen that the change of wall thickness has an effect on the maximum wall thickness reduction rate of pipes, but the influence range is limited. With the increase in eccentricity, the maximum elliptic rate of different wall thickness of the pipe changes in the magnitude of larger, when the pipe wall thickness of 1 mm, 10 mm eccentricity under the maximum elliptic rate of more than 8%, when the pipe wall thickness of 2mm, 8mm eccentricity under the maximum elliptic rate of more than 10% of the bend, that is, the bend produces more serious defects.

In summary, it can be seen that, under the same process parameters, the bending radius increases with the increase in wall thickness, the required Z-axis thrust and X-axis thrust is also the larger, with the increase in wall thickness of the pipe, the maximum wall thickness of the pipe thinning rate increases, the maximum ellipticity increases, the quality of pipe molding decreases.

3.3 Analysis of the Influence of Different Material Pipes on the Molding Law

There are great differences in the mechanical property parameters of metal pipes of different materials, and there are great differences in forming parameters such as bending angle, bending forming limit, rebound, ellipticity, wall thickness change rate, and so on in the pipe bending process. In this paper, TP2 copper pipes, Ta1 pipes, and 6061 aluminum alloy pipes were selected, respectively. Pipe outer diameter φ12mm, wall thickness 1 mm for finite element analysis, three different materials under the pipe bending and forming law to study, through the tensile test to obtain the material parameters of the three materials as shown in Table 2.

Fig. 7 shows the three pipe bending radius change schematic, when the eccentricity distance is 10 mm, 6061-AL pipe appears serious distortion cannot be formed normally. Theoretically, the greater the yield strength, indicating that the pipe resistance to plastic deformation ability, the lower the yield strength, the better the cold forming performance of the pipe will be. The lower the yield strength, the better the pipe cold forming performance will be. Then the same bending force, the greater the yield strength of the material, the larger the pipe bending radius. Young's modulus is a physical quantity that describes the ability of a solid material to resist deformation, this parameter can indicate the rigidity of the material, the greater the rigidity, the less likely to deform. Therefore, the larger the Young's modulus of the material, the larger the bending radius of the pipe. However, in the actual bending process, the bending radius of the three kinds of bends did not show a theoretical regular change, which can be speculated that the size of the bending radius of the pipe is not only determined by the modulus of elasticity and yield strength. Parameters such as the hardening index and strength coefficient of the pipe may also influence the bending radius of the pipe, and under the effect of multi-parameter coupling, the pipes of different materials show no regular change under the three eccentricity distances.

Table 2. Material properties of three metal tubes

Material	Density（tonne/mm^3）	Modulus of elasticity（GPa）	Yielding strength（MPa）	Tensile strength（MPa）	Poissonbee	Hardening index n
TP2 pipe	$8.94*10^{-9}$	115	33.48	376.87	0.31	0.6321
Ta1 pipe	$4.5*10^{-9}$	105	187.14	456.26	0.34	0.6561
6061-AL pipe	$2.7*10^{-9}$	69	253.73	347.44	0.33	0.0982

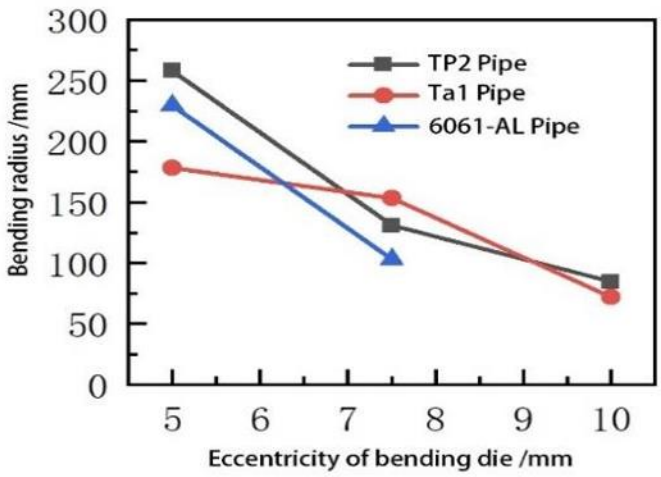

Fig. 7. Comparison of bending radius of different tubes

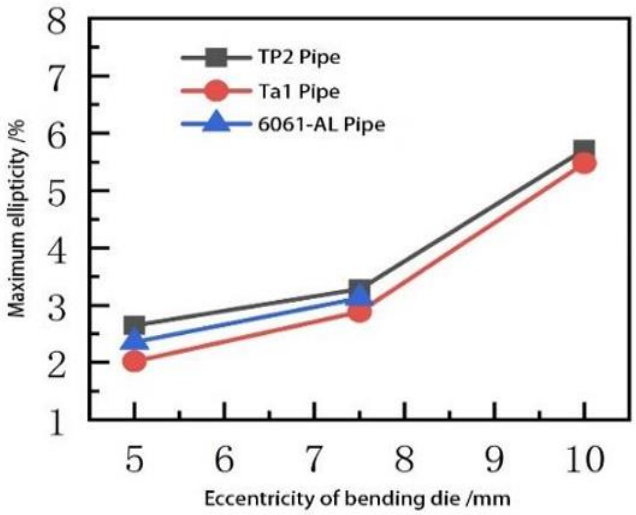

(a)

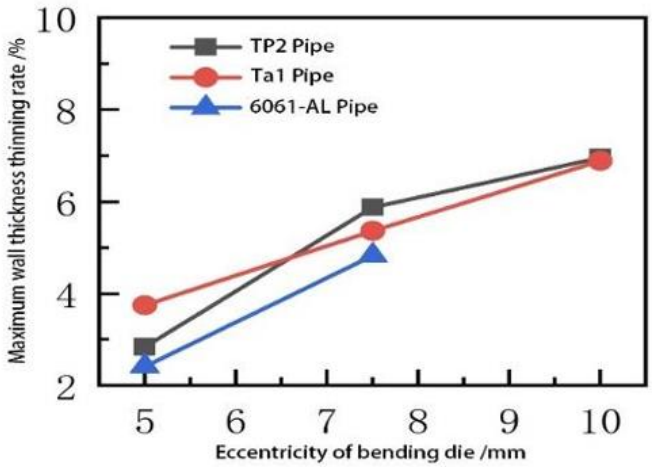

(b)

Fig. 8. Variation of maximum change rate of different tubes with eccentricity

The variation of maximum wall thickness reduction and maximum ellipticity for different pipes is shown in Fig. 8. It can be seen from Fig. 8a that the maximum ellipticity of different pipes increases with the increase in bending die eccentricity distance. From the lateral comparison of different pipes, the maximum ellipticity of Ta1 pipe is the lowest and TP2 pipe is the highest under the same bending die eccentricity distance. This is because the greater the strength of the material, the greater the ability of the material to resist the deformation of the cross-section, TP2 pipe yield strength is much lower than the Ta1 pipe and 6061-AL pipe, tensile strength is slightly higher than the 6061-AL pipe and with the Ta1 pipe is a large difference, and thus the maximum ellipticity of the TP2 pipe is the largest of the three tubes. The yield strength of Ta1 pipe is lower than that of 6061-AL pipe, but the tensile strength is higher than that of 6061-AL pipe. Taken together, the Ta1 pipe is stronger and therefore has a lower maximum ellipticity than the 6061-AL pipe.

From Fig. 8b, it can be seen that maximum wall thinning rate of different pipes increases with the increase of eccentricity, and the maximum wall thinning rate of TP2 pipe is higher than that of Ta1 pipe at the bending die eccentricity of 7.5 mm and 10 mm. This is due to the change in wall thickness of the pipe by the hardening index n, the hardening index is high, the material hardening effect is strong, the ductility of the material is also increased, according to the principle of incompressibility of the material, the pipe in the tangential strain increases, the maximum wall thickness of the thinning rate also increases. The hardening index of TP2 pipe is slightly higher than Ta1 pipe, so the maximum wall thickness reduction rate of TP2 pipe is larger under the same eccentricity, and the hardening index of 6061-AL pipe is much lower than that of other materials, so the maximum wall thickness reduction rate is the lowest among the three materials. However, the maximum wall thickness reduction rate of TP2 tubes is smaller than that of Ta1 tubes when the bending mode eccentricity is 5mm, which may be due to the fact that the bending radius of TP2 tubes is larger than that of Ta1 tubes when the eccentricity is 5mm, which leads to a reduction in the maximum wall thickness reduction rate.

4. MULTI-PARAMETER PIPE FORMING QUALITY ANALYSIS AND OPTIMIZATION BASED ON ORTHOGONAL TEST

The forming results of metal pipe bending are often subject to the coupling effect between multiple factors, in order to analyze the coupling effect of each parameter on the pipe forming influence law, this paper selects the bending die and pipe clearance value, the bending die fillet radius value, the length of pipe bending deformation zone, the guide mechanism fillet radius value, the guide mechanism and the pipe clearance value of the five-factor, three-level orthogonal experimental design to study the importance of the influence of each factor on the quality of the pipe and parameter optimization, the orthogonal table header design shown in Table 3, the orthogonal table header design. The importance of the influence of each factor on the quality of pipe forming and parameter optimization [14], orthogonal table header design is shown in Table 3.

Find the standard orthogonal table according to the selected factors and levels, and select Table L_{27} (3^5) in the standard orthogonal table for the 27-group orthogonal experimental design. The five test factors were replaced by ABCDE and the different levels were replaced by 123, so that each group of test solutions can be expressed by a combination of letters ABCDE and numbers 123, respectively, and simulation analysis was carried out with the 27 groups of orthogonal tests designed in section 3.2, and the results of the simulation data are shown in Table 4.

In order to intuitively find out the magnitude and significance of the influence of each factor on the pipe forming quality, the extreme difference analysis method was chosen to process the finite element simulation results. As can be seen from Table 5 of the polar analysis, the influence of each parameter on the quality of pipe forming is as follows: guide mechanism and pipe gap E > bending deformation zone length C > bending die fillet radius B > guide mechanism fillet radius D > pipe die gap A.

ANOVA can distinguish differences between test results from error fluctuations, can validate the accuracy of the results of the polar analysis method, and determine the significance of the effect of each factor on the indicator.

Table 3. Design factors level table of free bending orthogonal test

Level	Factors				
	A Pipe mold clearance（mm）	B Bending die corner radius（mm）	C Bending deformation zone length（mm）	D Guide mechanism corner radius（mm）	E Guide mechanism and pipe clearance value（mm）
1	0.1	1.5	21	1.5	0.2
2	0.2	2	23	2	0.3
3	0.3	2.5	25	2.5	0.4

Table 4. Simulation results

Trail No.	Factors			
	Pilot programs	Maximum wall thickness reduction（%）	Maximum ellipticity（%）	Optimization results of the efficacy coefficient method
1	A1B1C1D1E1	5.04	3.08	0.552
2	A1B1C1D1E2	5.18	3.47	0.526
3	A1B1C1D1E3	4.7	6.82	0.280
4	A1B2C2D2E1	4.7	5.89	0.374
5	A1B2C2D2E2	4.39	5.54	0.415
6	A1B2C2D2E3	3.85	6.26	0.366
7	A1B3C3D3E1	4.23	5.95	0.385
8	A1B3C3D3E2	4.02	6.76	0.304
9	A1B3C3D3E3	3.49	7.85	0.110
10	A2B1C2D3E1	4.86	4.21	0.493
11	A2B1C2D3E2	4.41	5.54	0.415
12	A2B1C2D3E3	4.1	6.20	0.364
13	A2B2C3D1E1	4.28	5.67	0.408
14	A2B2C3D1E2	3.87	6.67	0.319
15	A2B2C3D1E3	3.65	7.65	0.167
16	A2B3C1D2E1	5.24	5.33	0.399
17	A2B3C1D2E2	4.93	4.28	0.486
18	A2B3C1D2E3	4.44	5.38	0.427
19	A3B1C3D2E1	4.22	5.86	0.393
20	A3B1C3D2E2	3.79	6.81	0.304

Trail No.	Factors			
	Pilot programs	Maximum wall thickness reduction（%）	Maximum ellipticity（%）	Optimization results of the efficacy coefficient method
21	A3B1C3D2E3	3.41	6.22	0.383
22	A3B2C1D3E1	5.52	5.15	0.399
23	A3B2C1D3E2	4.88	4.13	0.498
24	A3B2C1D3E3	4.45	6.74	0.296
25	A3B3C2D1E1	6.67	3.92	0.412
26	A3B3C2D1E2	4.23	5.98	0.382
27	A3B3C2D1E3	3.98	7.12	0.257

Table 5. Range analysis

Index	Factors				
	Pipe mold clearance（mm）	Bending die corner radius（mm）	Bending deformation zone length（mm）	Guide mechanism corner radius（mm）	Guide mechanism and pipe clearance value（mm）
K1	0.3680	0.4122	0.4292	0.3670	0.4239
K2	0.3864	0.3602	0.3864	0.3941	0.4054
K3	0.3693	0.3513	0.3081	0.3627	0.2944
R	0.0184	0.0609	0.1211	0.0314	0.1294

Table 6. Analysis of variance

Source	*df*	SS	MS	F	P(%)
Pipe mold clearance（mm）	2	0.001904	0.000952	0.19	0.826
Bending die corner radius（mm）	2	0.019471	0.009736	1.97	0.171
Bending deformation zone length（mm）	2	0.067902	0.033951	6.89	0.007
Guide mechanism corner radius（mm）	2	0.005228	0.002614	0.53	0.599
Guide mechanism and pipe clearance value（mm）	2	0.088251	0.044126	8.95	0.002
Inaccuracies e	16	0.078894	0.004931		
Aggregate T	26	0.261651			

According to the results of ANOVA in Table 6, it can be seen that factor E and factor C have the most significant effect and factors A, B, and D have insignificant effects at a significance level of 0.1. Therefore, when selecting the parameters, the optimal value of the gap between the guiding mechanism and the pipe and the length of the bending deformation zone, E1C1, is selected in priority, followed by the selection of a more appropriate radius of the bending die fillet and the radius of the guiding mechanism fillet according to the results of the analysis of the extreme variance, and then the selection of the value of the pipe die gap, A, is considered in the end. At the same time, it can be seen through the ANOVA analysis that the results of the ANOVA analysis are consistent with the results of the extreme variance analysis.

5. EXPERIMENTAL STUDY OF FREE BENDING MOLDING

The direction of motion of the three-axis free bending equipment is shown in Fig. 9. In the X/Y plane, under the action of two servo motors, spherical bearings on the panel through the ball screw on two sets of linear guideways to achieve plane movement. z-axis direction, the actuator through the ball screw drive to push the pipe toward the Z-axis direction to ensure that the transmission under the action of servo motors has a high degree of accuracy.

Fig. 9. Three axis movement direction of free bending equipment

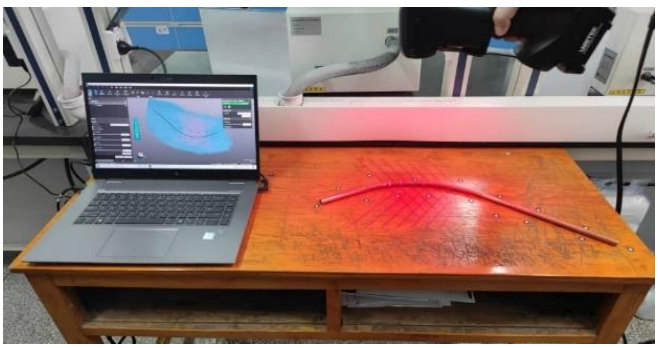

Fig. 10. Handheld 3D digital scanner

For the post-processing of this free bending and forming test, a handheld 3D digital scanner was used to scan the pipe in 3D after bending and forming, and the scanning equipment is shown in Fig. 10.

Select φ12 * 1mm TP2 copper pipe as the test material, guide mechanism and pipe clearance 0.2mm, pipe bending deformation zone length of 40mm, bending die corner radius 2mm, guide mechanism corner radius 2mm, bending die and pipe clearance 0.2mm, in order to reduce friction in the test process of the pipe, in the pipe on the outer surface of the lubricating oil. Three groups of different pipe bending tests were carried out, and the specific test parameters are shown in Table 7.

Under three sets of parameters, free bending forming tests and free bending finite element simulation were carried out, and the three sets of test results were compared with the simulation results, respectively, and the free bending test results and simulation results are shown in Fig. 11.

Table 7. Design parameters of three-dimensional free bending experiment

Parameters	No. of groups		
	Group 1	Group 2	Group 3
Rate of advance（mm/s）	70	50	50
Spherical bearing eccentricity (mm)	5	7	9
First transition time (s)	1	2	2
Arc time (s)	3	3	3
Second transition period (s)	1	2	2
Pipe deformation length (mm)	350	350	350

Fig. 11. comparison between experiment and simulation

Table 8. Comparison results of test simulation

	Bending radius (mm)	Bending angle (mm)		Maximum wall thickness reduction (%)	Maximum ellipticity (%)
Trial 1	329.16	35.45	**Trial 1**	1.66	1.81
Analog 1	322.55	37.17	**Analog**	1.83	1.02
Deviation rate	2.01%	4.63%	**Deviation**	0.17%	0.79%
Trial 2	277.03	43.95	**Trial 2**	2.02	3.77
Analog 2	267.32	46.21	**Analog 2**	2.66	3.04
Deviation rate	3.51%	4.89%	**Deviation**	0.64%	0.73%
Trial 3	192.23	65.68	**Trial 3**	4.82	5.76
Analog 3	184.33	69.08	**Analog 3**	5.22	4.61
Deviation rate	4.11%	4.92%	**Deviation**	0.4%	1.15%

The bending angle, bending radius, maximum wall thickness reduction rate, maximum elliptic rate of the above results were analyzed, and the comparison results are shown in Table 8, the bending angle and bending radius deviation of the pipe in the test and simulation values increase with the increase of the bending die eccentricity, but the deviation of the bending angle and bending radius values of the three test results and the simulation results are less than 5%, which is a high degree of consistency. The deviation values of maximum wall thickness reduction and maximum ellipticity of the pipe are lower than 2%, and the maximum wall thickness reduction of the pipe is lower than 10% and the maximum ellipticity of the pipe is lower than 8% in the three tests and simulations, which have better forming quality.

The reason for the deviation between the test results and the simulation results may be caused by the friction change during the movement of the pipe in the actual test, the temperature change, the different clearance between the bending die and the spherical bearing, and the existence of bending springback of the pipe. Therefore, this three-axis free bending and forming equipment can realize accurate pipe bending and forming, and at the same time, the finite element simulation can provide a reliable basis for the actual forming test.

6. CONCLUSION

(1) Based on the three-axis free bending equipment to analyze the principle of three-axis free bending and establish a mechanical model. TP2 copper pipe as the main research object, to determine the maximum wall thickness reduction rate of the pipe and the maximum elliptic rate as the evaluation index of pipe forming quality, determine the efficacy coefficient method as the multi-objective optimization method in this paper.

(2) By studying pipes with different wall thicknesses, it is found that wall thickness affects the bending radius of the pipe, and the smaller the bending radius, the more significant the effect. As the wall thickness of the pipe increases, the pipe forming quality decreases. Through the study of different materials of pipe found that the pipe bending radius size is determined by the material modulus of elasticity, yield strength, pipe hardening index and strength factor and other parameters. The maximum ellipticity of the pipe is related to the strength of the material and the variation in wall thickness of the pipe is influenced by the hardening index n.

(3) Orthogonal tests are designed according to five process parameters, and the pipe forming quality is analyzed and optimized by extreme difference analysis and analysis of variance (ANOVA). The analysis shows that the influence of each parameter on the quality of pipe forming is as follows: guide and pipe gap E > bending deformation zone length C > bending die radius B > guide radius D > pipe die gap A. The guide and pipe gap E and bending deformation zone length C have the most significant influence on the quality of pipe forming, and they should be given priority in the actual test. The bending test is carried out using three-axis free bending equipment and compared with the finite element simulation results. From the three comparisons, the difference between the finite element simulation results and the actual test results is relatively small, and the optimization results of the orthogonal test are of great significance in improving the quality of pipe forming and the improvement of the forming mechanism of the test equipment.

DISCLAIMER (ARTIFICIAL INTELLIGENCE)

Author(s) hereby declare that NO generative AI technologies such as Large Language Models (ChatGPT, COPILOT, etc) and text-to-image generators have been used during writing or editing of manuscripts.

COMPETING INTERESTS

Author has declared that no competing interests exist.

REFERENCES

1. Hermes M, Staupendahl D, Becker C, et al. Innovative machine concepts for 3D bending of tubes and profiles [J]. Key Engineering Materials. 2011;473:37-42.
2. Cheng X, Zhao Y, Abd El-Aty A, et al. Deformation behavior of convolute thin-walled AA6061-T6 rectangular tubes manufactured by the free bending forming technology[J]. The International Journal of

Advanced Manufacturing Technology. 2022;1-16.

3. Cheng C, Wei G, Zhang H, et al. Theoretical analysis, finite element modeling and experimental investigation of the impact of friction between tube and bending die on the formability of the tube during the free-bending process [J]. CIRP Journal of Manufacturing Science and Technology. 2023;44:104-115.
4. Zhang Z, Wu J, Liang B, et al. Investigation to the torsion generation of spatial tubes in bending-twisting process [J]. International Journal of Advanced Manufacturing Technology. 2020;(4):1-13.
5. Wu J, Zhang Z. An improved procedure for manufacture of 3D tubes with springback concerned in flexible bending process [J]. Chinese Journal of Aeronautics; 2020.
6. Wfang Jun, Ouyang Fang, Shang Wenxuan, et al. Influence of process parameters on the springback behavior of high-strength stainless steel tubes under the condition of elastic modulus change[J]. Forging Technology. 2023;47(11):137-145(in Chinese).
7. Guo X Z, Yang Q C, Cheng C, Liu C M, Xu Y, Bai X S, Li G J. Research on six-axis free bending forming mechanism and forming quality control of profile components [J]. Aeronautical Manufacturing Technology. 2022;65(10): 24-32(in Chinese).
8. Yu Bo, Shu Sai, Cheng Zonghui, et al. Study on the influence law of friction effect on the deformation behavior of pipe in three-dimensional free bending process[J]. Journal of Weapons and Equipment Engineering. 2023;44(02):203-210(in Chinese).
9. MA Y N, XIONG H, WANG H, et al. Simulation and experimental study on three dimensional free bending of complex space elbow[J]. Journal of Netshape Forming Engineering, 2017, 9(02):20-26(in Chinese).
10. E D X, Zhou D J. Metal tube bending: theory and forming defects analysis [M]. Beijing: Beijing Institute of Technology Press; 2016 (in Chinese).
11. Hao Yongxing, Zhang Shaohua, Liu Yahui. Research on three-dimensional free bending forming rule of pipe based on numerical simulation [J]. Manufacturing automation, 2021, 43 (11): 101-104（in Chinese）.
12. WANG T H. Plastic processing technology of pipes [M]. Beijing: China Machine Press,1998:30-33 (in Chinese).
13. TANG H W, QIN X Z. Practical methods of optimization [M]. 3rd ed. Dalian: Dalian University of Technology Press,2004(in Chinese).
14. HE W, TANG B, XUE W D, et al. Optimization design of experiment and data analysis[M]. Beijing: Chemical Industry Press,2012(in Chinese).

Disclaimer/Publisher's Note: The statements, opinions and data contained in all publications are solely those of the individual author(s) and contributor(s) and not of the publisher and/or the editor(s). This publisher and/or the editor(s) disclaim responsibility for any injury to people or property resulting from any ideas, methods, instructions or products referred to in the content.

© Copyright (2024): Author(s). The licensee is the journal publisher. This is an Open Access article distributed under the terms of the Creative Commons Attribution License (http://creativecommons.org/licenses/by/4.0), which permits unrestricted use, distribution, and reproduction in any medium, provided the original work is properly cited.

Peer-review history:
The peer review history for this paper can be accessed here:
https://www.sdiarticle5.com/review-history/120556